

## **Water mass structure defines the diapausing copepod distribution in a right whale habitat on the Scotian Shelf**

**Kimberley T. A. Davies<sup>1\*</sup>, Christopher T. Taggart<sup>1</sup>, R. Kent Smedbol<sup>1,2</sup>**

<sup>1</sup>Department of Oceanography, Dalhousie University, 1355 Oxford St. Halifax, Nova Scotia, B3H 4R2, Canada

<sup>2</sup>Fisheries and Oceans Canada, Bedford Institute of Oceanography, 1 Challenger Drive, Dartmouth, Nova Scotia, B2Y 4A2, Canada

\*Email: kim.davies@dal.ca

*Marine Ecology Progress Series 497:69–85 (2014)*

---

### **Supplement. Calibration of TUBSS optical plankton counter (OPC) using BIONESS OPC**

Regression analysis comparing the BIONESS net and BIONESS OPC plankton energy densities collected in 2008 to 2009 was used to calibrate the TUBSS OPC in 2008. The calibration was based on data from 19 net samples collected at 4 stations in 2008, and from 14 net samples at 3 stations in 2009. BIONESS data are available in the supplementary material of Davies et al. (2013) (see main text for source literature).

First, random samples of CH4s and CF5s ( $n = 54$  to  $274$ ) were sorted from each deep ( $>75$  m) net collection, photographed from the lateral view, and prosome lengths and widths measured digitally. Next, CH4 and CF5 prosome volumes were estimated from length and width using a geometric shape approximation for an oblate spheroid, and the ESD of CH4s and CF5s from the net collections ( $ESD_{net}$ ) was estimated from prosome volume. Because the abundance-at-size distribution measured by the OPC reflects a combination of overlapping CH4 and CF5 size distributions without differentiating by species, we then combined the 2 species'  $ESD_{net}$  distributions, scaling the contribution of each species to all size classes using the average relative concentration over all deep nets. The animals were then classified into  $DS_{net}$  using the inverse of Eq. (1) (see main text) and converted into 64  $S_{net}$  size classes equivalent to  $S_{opc}$  above. The  $S_{net}$  distributions were normal (2009) or slightly right-skewed (2008) and varied over the same size range in both years, corresponding to  $S_{net}$  bin classes 7 to 14 that have geometric mean ESD between 761 and 1630  $\mu\text{m}$  (Fig. S1). The combined distribution was slightly right-skewed (though still fairly normal) in 2008 because the larger CH4 was present in high abundance relative to CF5 (CF5:CH4 in 2008; 80:20%, Fig. S2). The distribution was normal in 2009 because it was dominated by CF5 (CF5:CH4 in 2009; 95:5%, Fig. S2). The combined  $S_{net}$  distribution provided the size frequency estimates for CH4s and CF5s to be selected from the wider  $S_{opc}$  size frequency distribution (Fig. S2). The  $S_{opc}$  distribution was shifted to larger size classes (9 to 16) relative to the  $S_{net}$  in both years.

The  $S_{opc}$  classes were shifted upward by 2 size classes relative to  $S_{net}$  classes, so when we applied the energy terms to the OPC-abundance-at-size distribution, we multiplied energy content from  $S_{net}$  class 7 with abundance from  $S_{opc}$  class 9, etc. We then integrated the total energy (J) over  $S_{opc}$  classes 9 to 16, and the integrated data were summed over the BIONESS-net deployment period and divided by the total volume sampled by the OPC over the same period, to obtain net-specific BIONESS OPC energy density ( $\text{kJ m}^{-3}$ ). For each corresponding net, the total CH4 + CF5 concentration was divided proportionally into the size classes illustrated in Fig. S1, and energy

content was multiplied by the C4+C5 concentration in each  $S_{net}$  class and then summed over all  $S_{net}$  classes to obtain BIONESS net-derived energy density ( $\text{kJ m}^{-3}$ ). Linear regression was then applied to the 2 series to develop the calibration equation depicted in Fig. S3.

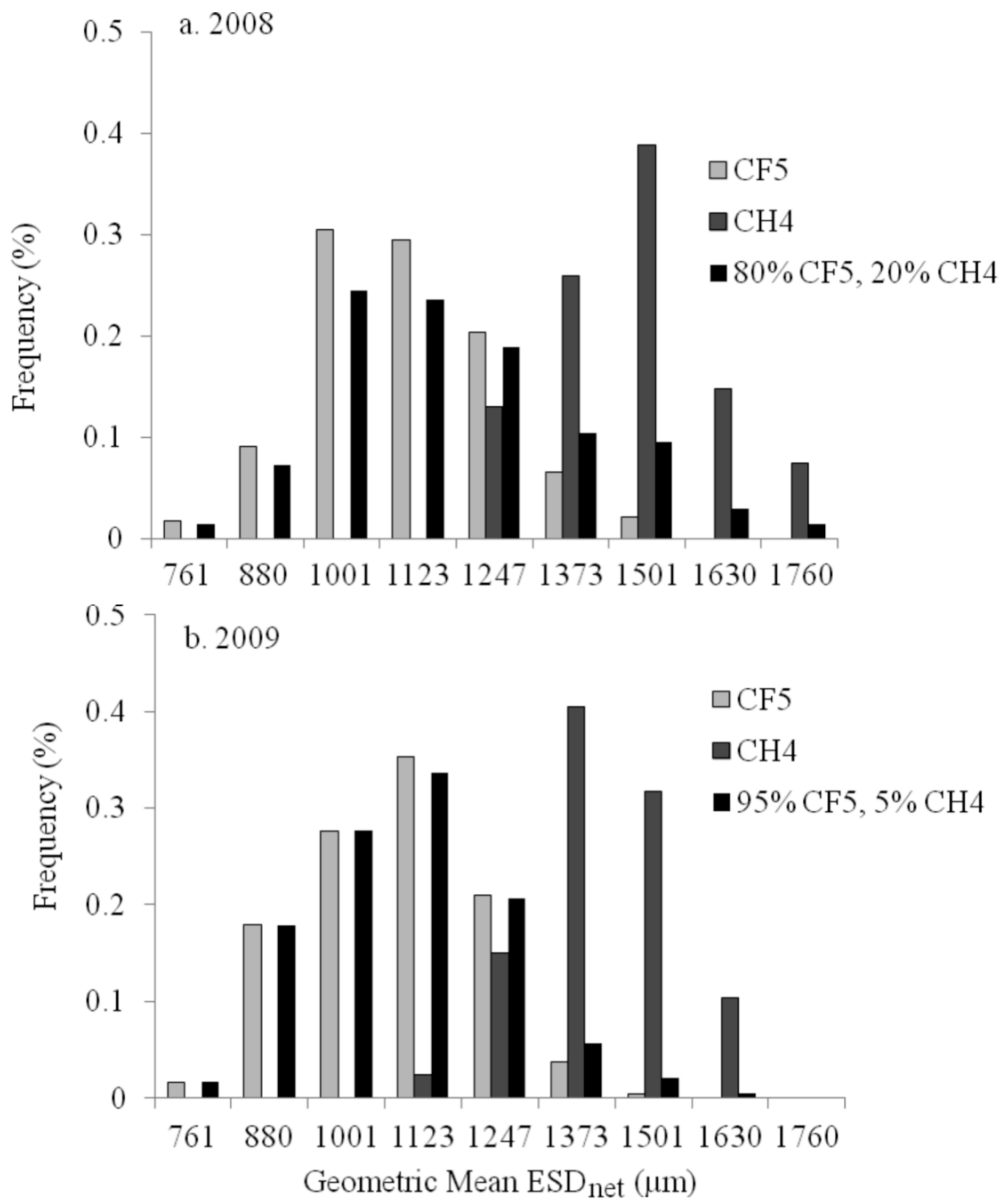


Fig. S1. ESD<sub>net</sub> ( $\mu\text{m}$ ) size frequency distributions of net-collected *Calanus finmarchicus* C5 (CF5, light grey bars) and *C. hyperboreus* C4 (CH4, dark grey bars) from the deep (>75 m) depth strata in September (a) 2008 and (b) 2009 where the sizes were determined from digital images of the copepods. The black bars represent the combined size distribution of both species, scaled by their relative proportional concentrations in the nets. The combined distribution is the size frequency distribution measured by the OPC

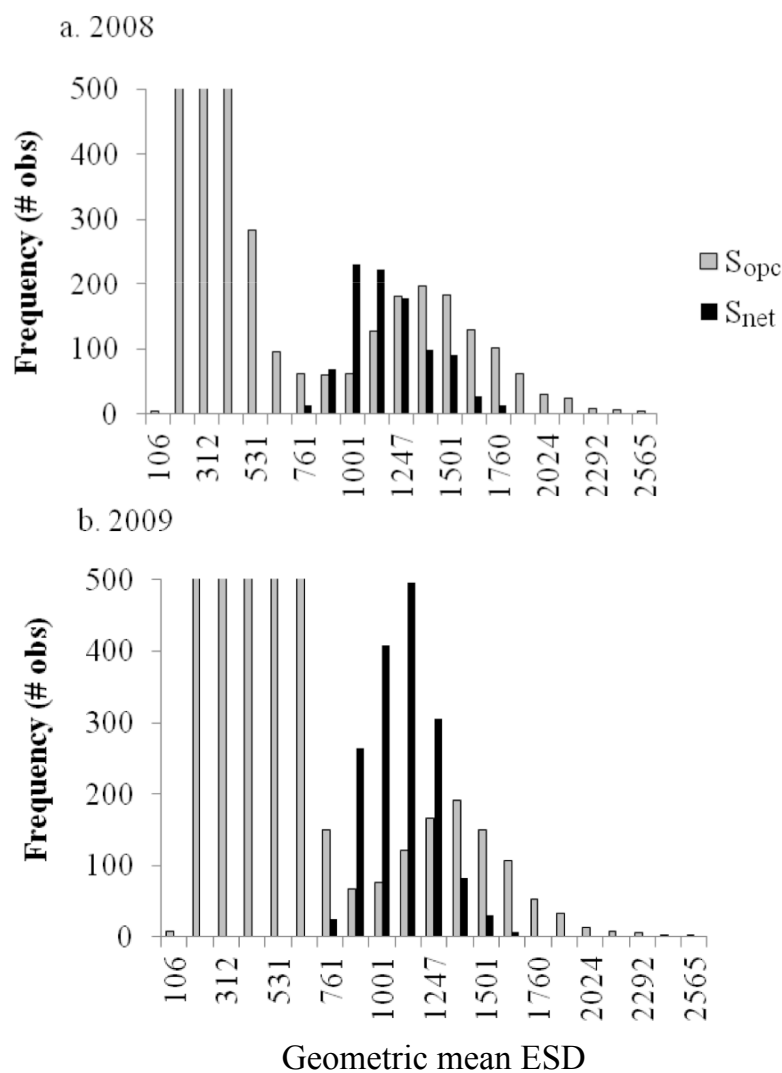


Fig. S2. BIONESS OPC-derived (grey) and BIONESS-net derived (black) concentration-at-size distributions collected simultaneously at (a) Stn B02 with net 5 (2008) or (b) Stn B02 with net 2 (2009). Biological samples fell within  $S_{net}$  bin classes 7 to 14 (mean ESD: 761–1630  $\mu\text{m}$ ), and the BIONESS OPC distributions were shifted relative to  $S_{net}$  toward larger size classes, ranging from 9 to 16 (mean ESD: 1001–1891  $\mu\text{m}$ ). The first 6 bins are cut off at 500 observations to enhance the ability to see the relevant size range. The first 6 bins contain small particles such as marine snow that are not relevant to the study

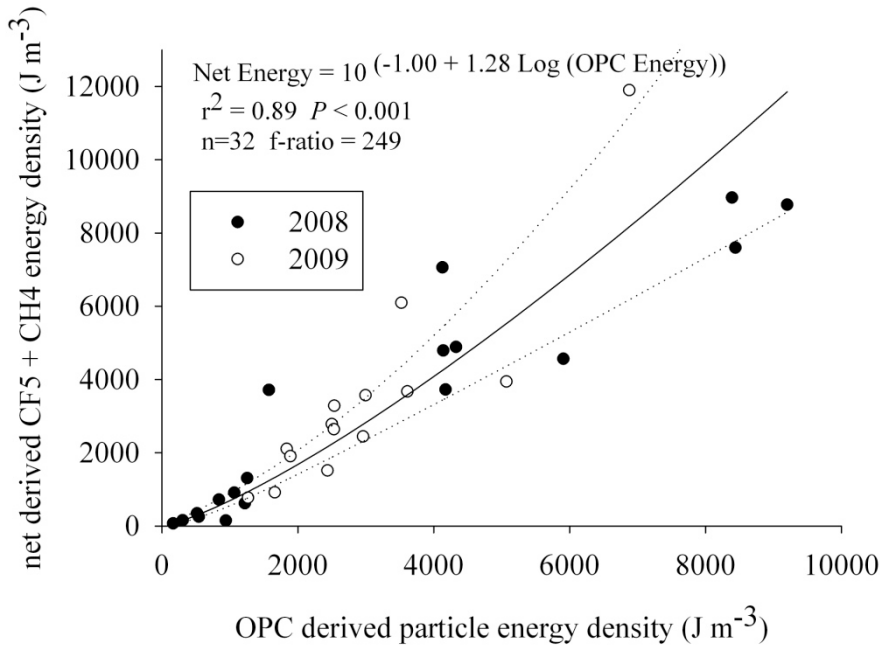


Fig. S3. Regression-based calibration of the BIONESS OPC and corresponding BIONESS net-derived *Calanus finmarchicus* CF5 and *C. hyperboreus* CH4 energy density, where dotted lines denote the 95% confidence intervals around the predictions. OPC-derived energy density was estimated as the sum of plankton between  $S_{\text{opc}}$  size classes 9 to 16 (mean ESD: 1001–1891  $\mu\text{m}$ ), multiplied by individual energy content and divided by the total OPC volume sampled over the net-sampling period

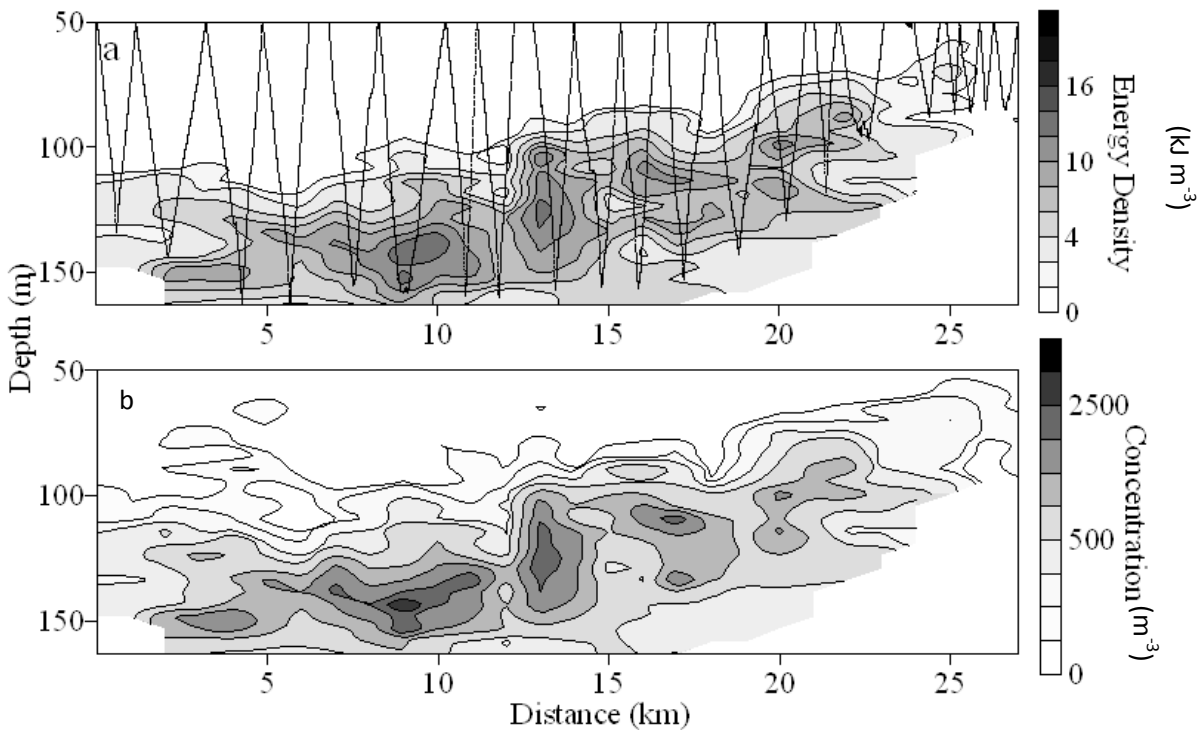


Fig. S4. Comparison between sectional distributions of diapausing copepod (a) energy density ( $\text{kJ m}^{-3}$ ) and (b) concentration ( $\text{m}^{-3}$ ) collected along transect-2. The TUBSS sampling path is shown with a zigzagged line in (a), and the transect's geographic position is shown in Fig. 1b in the main text. The blank regions at the bottom left and right of each panel represent the seafloor

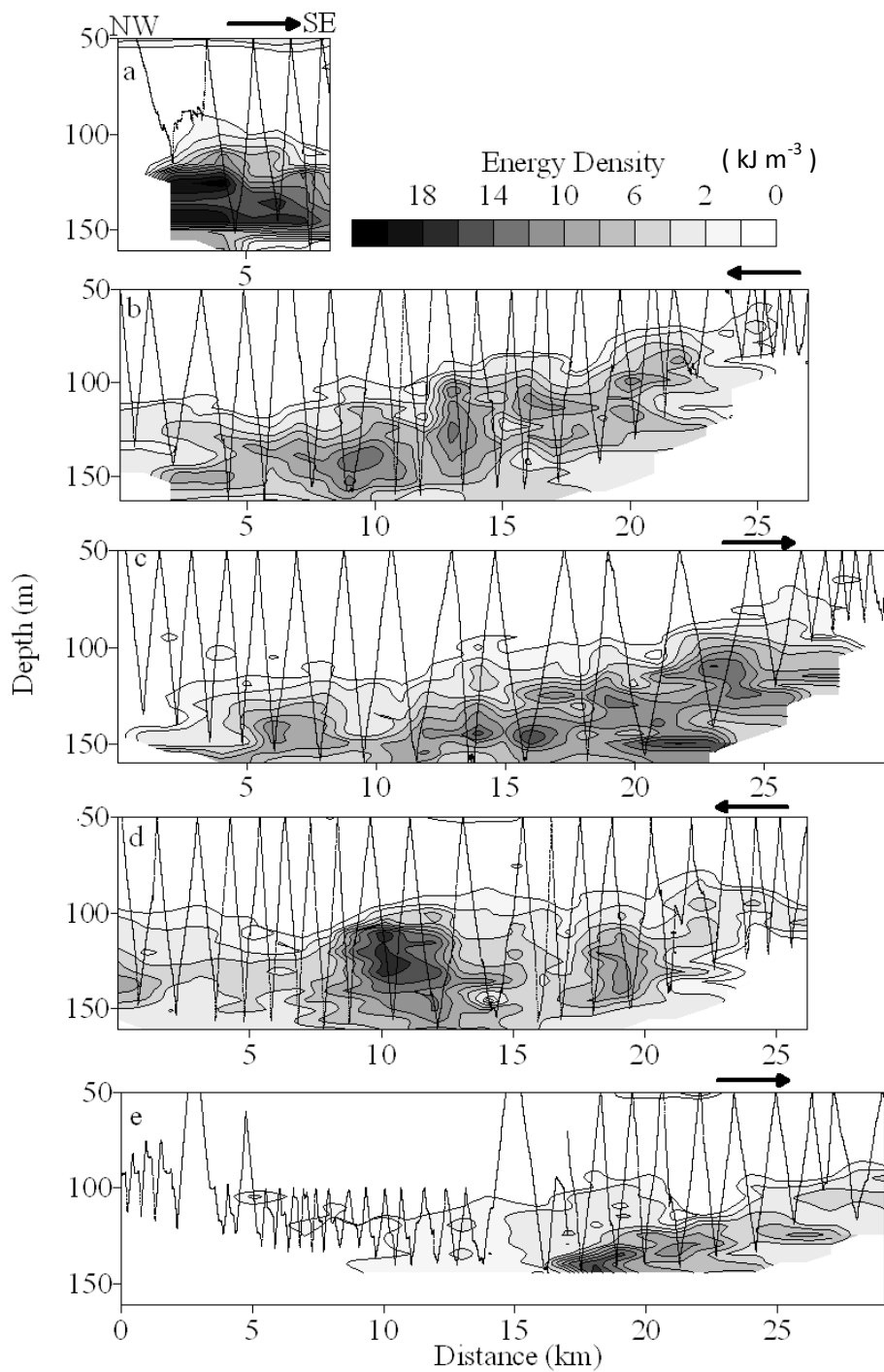


Fig. S5. Sectional distribution of copepod energy density ( $\text{kJ m}^{-3}$ ), estimated using the TUBSS-mounted OPC in September 2008 in Roseway Basin along the NW to SE transects-1 through -5 (a through e) shown in Fig. 1 in the main text. Arrows on each panel denote the direction of the tow, and zigzagged lines show the TUBSS tow profile. The blank regions at the bottom left and right of each panel represent the seafloor

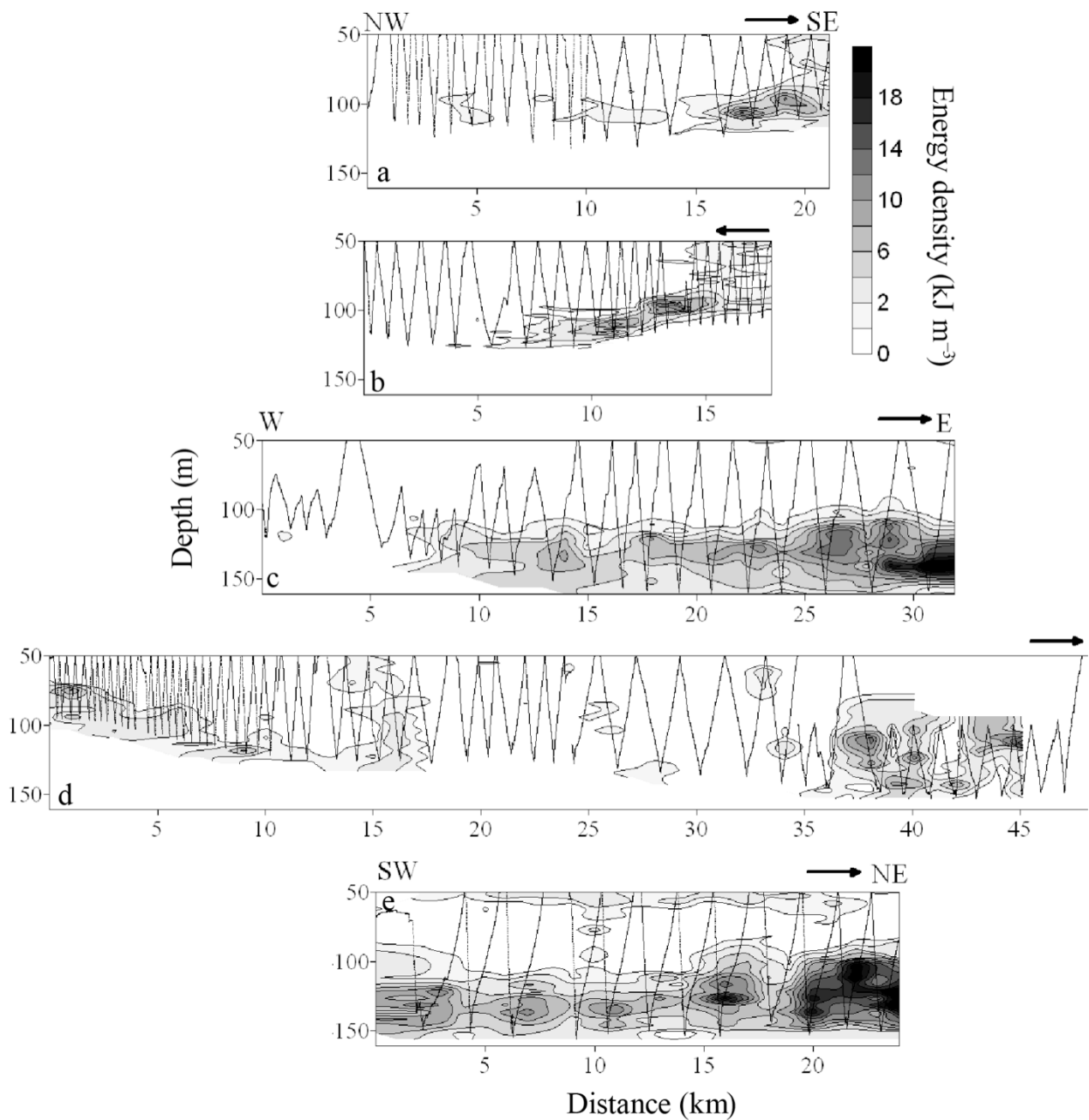


Fig. S6. Sectional distribution of copepod energy density ( $\text{kJ m}^{-3}$ ), estimated using the TUBSS-mounted OPC in September 2008 in Roseway Basin (a, b) along the NW to SE transects-6 and -7, (c, d) along the W to E transects-8 and -9, and (e) SW to SE along transect-10 (e). Arrows on each panel denote the direction of the tow, and zigzagged lines show the TUBSS tow profile. The blank regions at the bottom left and right of each panel represent the seafloor

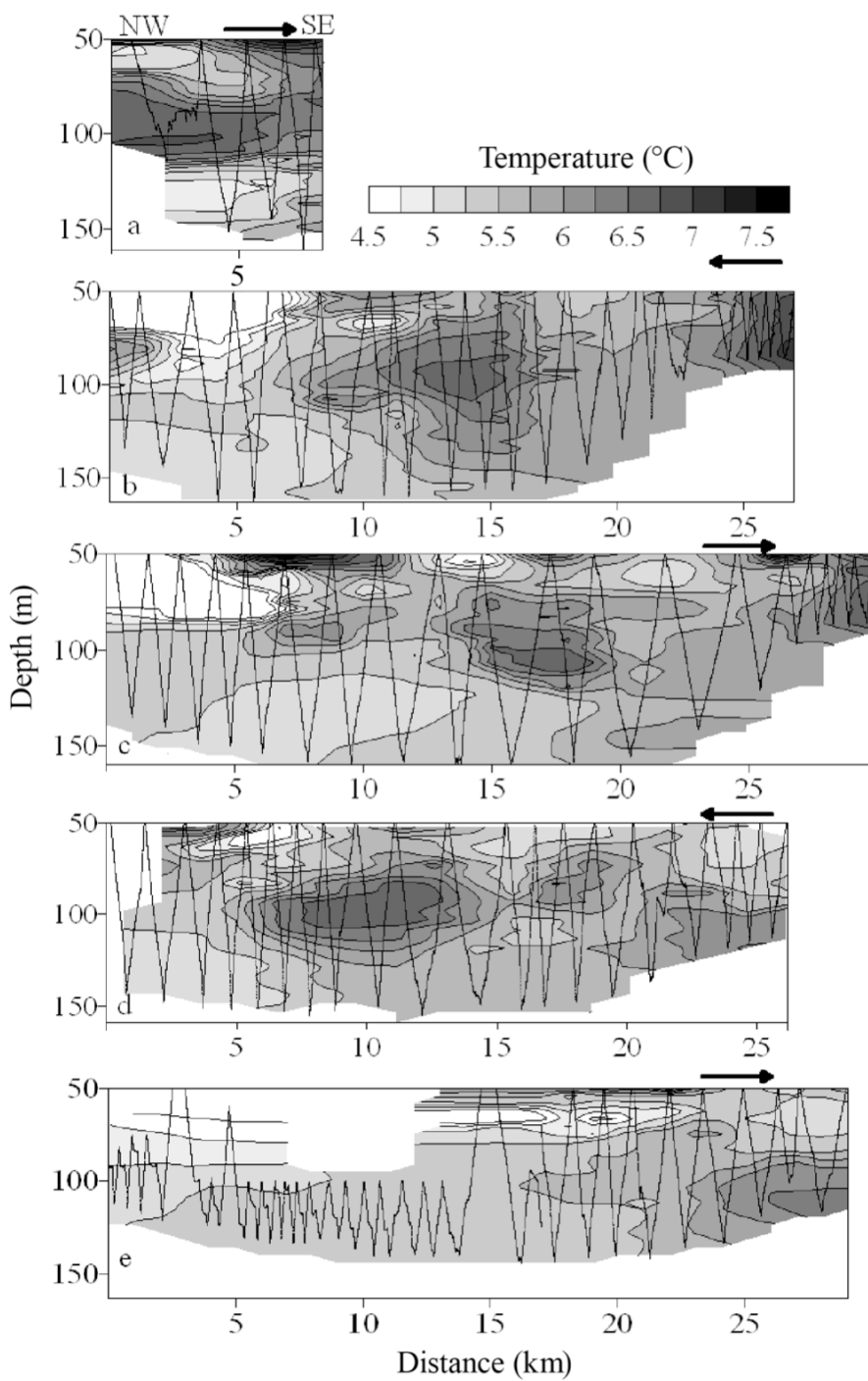


Fig. S7. Sectional distribution of temperature ( $^{\circ}\text{C}$ ), estimated using the TUBSS-mounted Seabird-37 CTD in September 2008 in Roseway Basin along the NW to SE transects-1 through -5 (panels a through e). Arrows on each panel denote the direction of the tow, and zigzagged lines show the TUBSS tow profile. Transect line locations are depicted in Fig. 1 in the main text

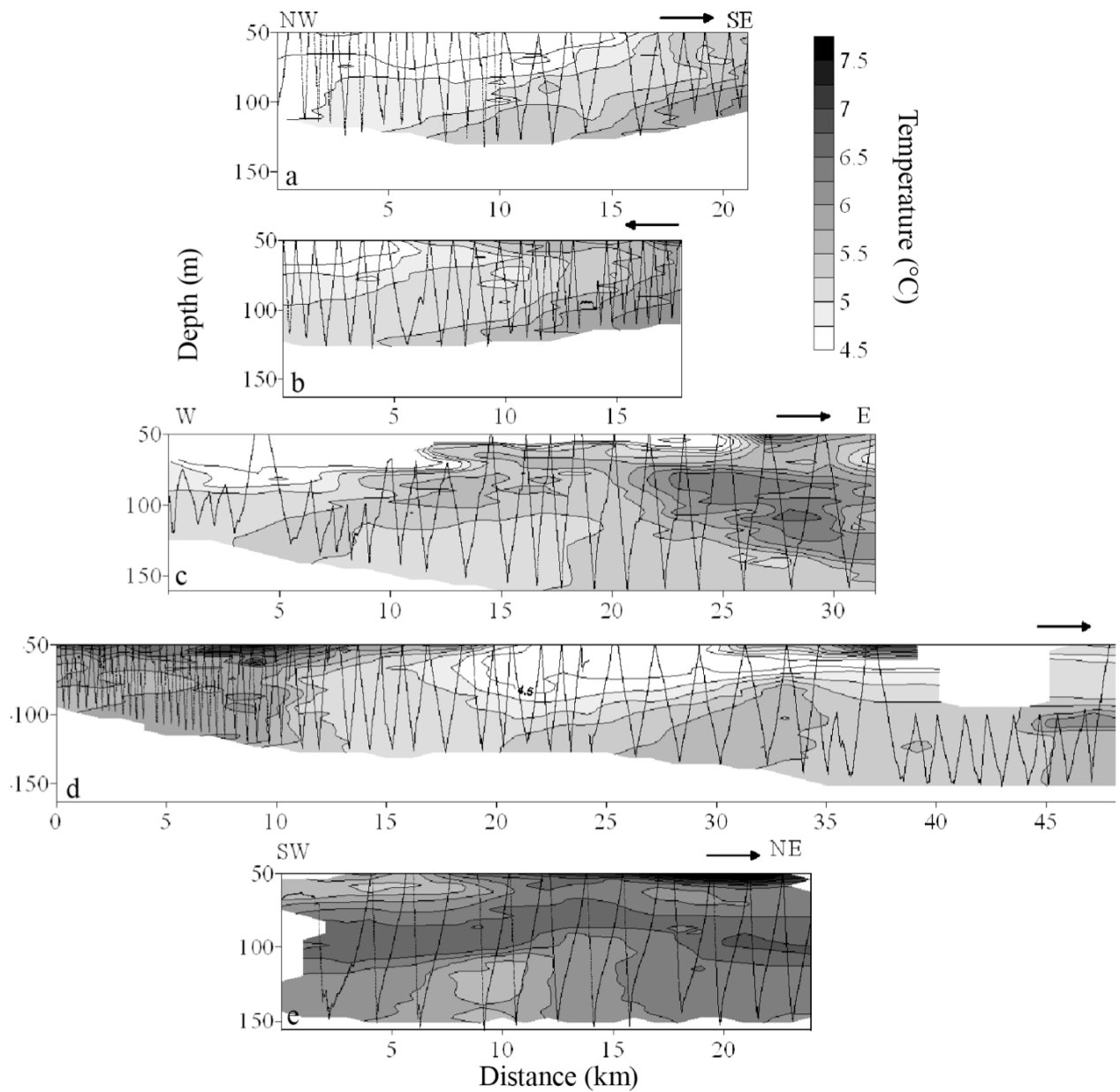


Fig. S8. Sectional distribution of temperature (°C), estimated using the TUBSS-mounted Seabird-37 CTD in September 2008 in Roseway Basin (a, b) along the NW to SE transects-6 and -7, (c, d) along the W to E transects-8 and -9, and (e) SW to SE along transect-10. Arrows on each panel denote the direction of the tow, and zigzagged lines show the TUBSS tow profile. Transect line locations are depicted in Fig. 1 in the main text

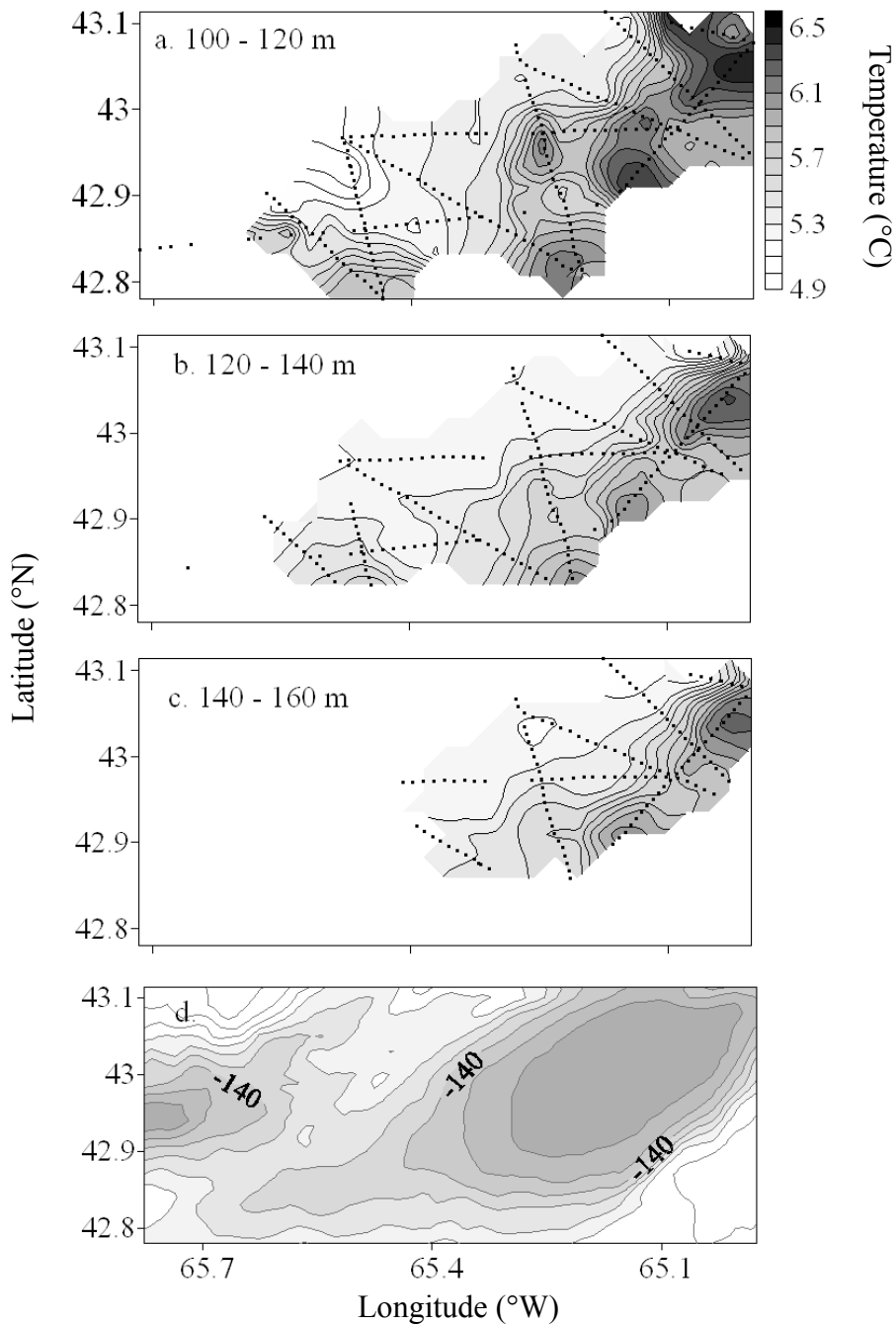


Fig. S9. Planar distribution of depth averaged water mass temperature (°C) in September 2008 in the Roseway Basin over (a) the 100–120 m stratum, (b) the 120–140 m stratum, and (c) the 140–160 m stratum, where the bathymetric contours (10 m intervals) are provided in (d). The data were derived from each transect (illustrated in Figs. S3 & S4). Each datum is indicated with black symbols. Where data are depicted without contours, the data were insufficient to make an interpolation

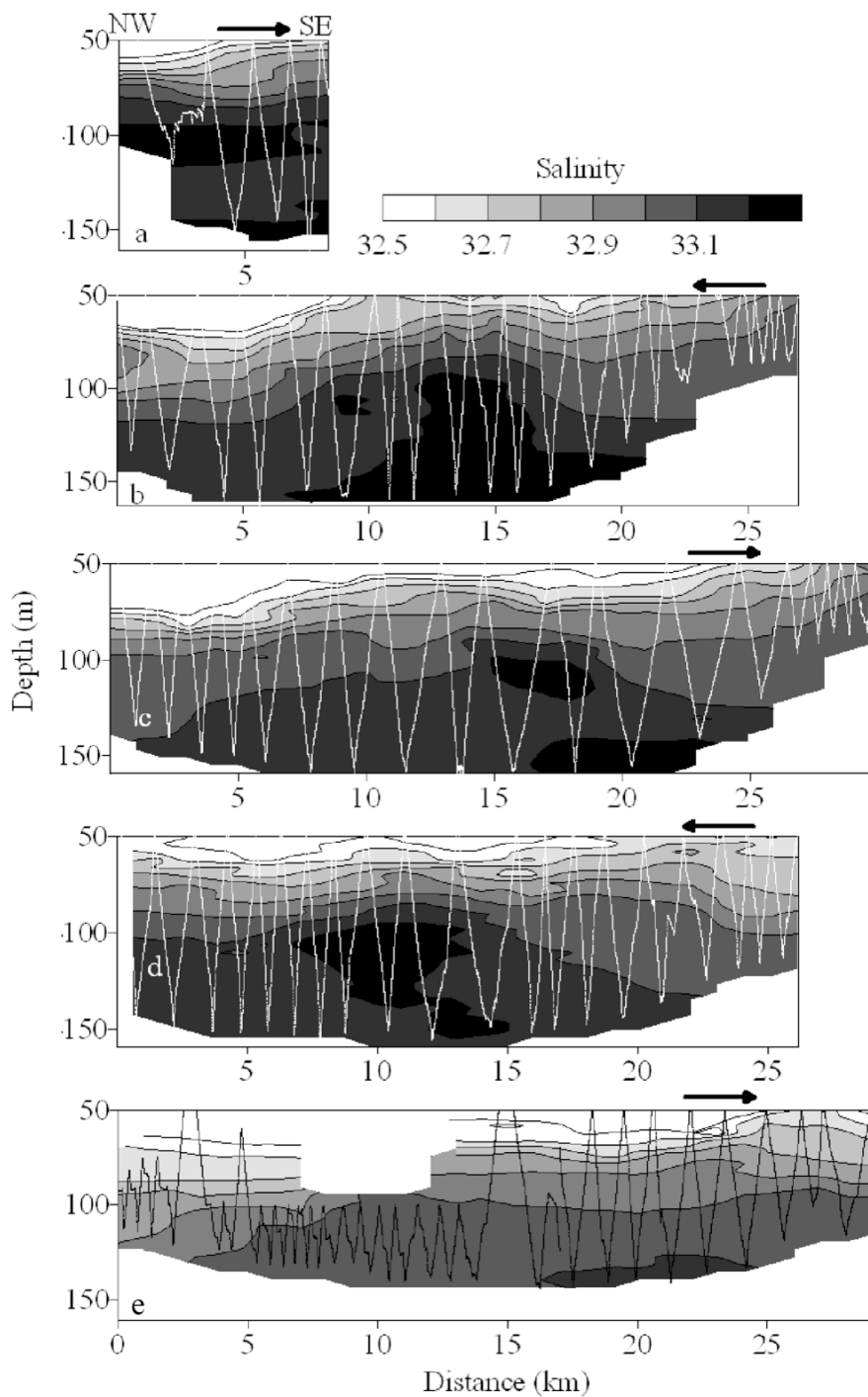


Fig. S10. Sectional distribution of salinity, estimated using the TUBSS-mounted Seabird-37 CTD in September 2008 in Roseway Basin along the NW to SE transects-1 through -5 (panels a through e). Arrows on each panel denote the direction of the tow, and zigzagged lines show the TUBSS tow profile. Transect line locations are depicted in Fig. 1 in the main text

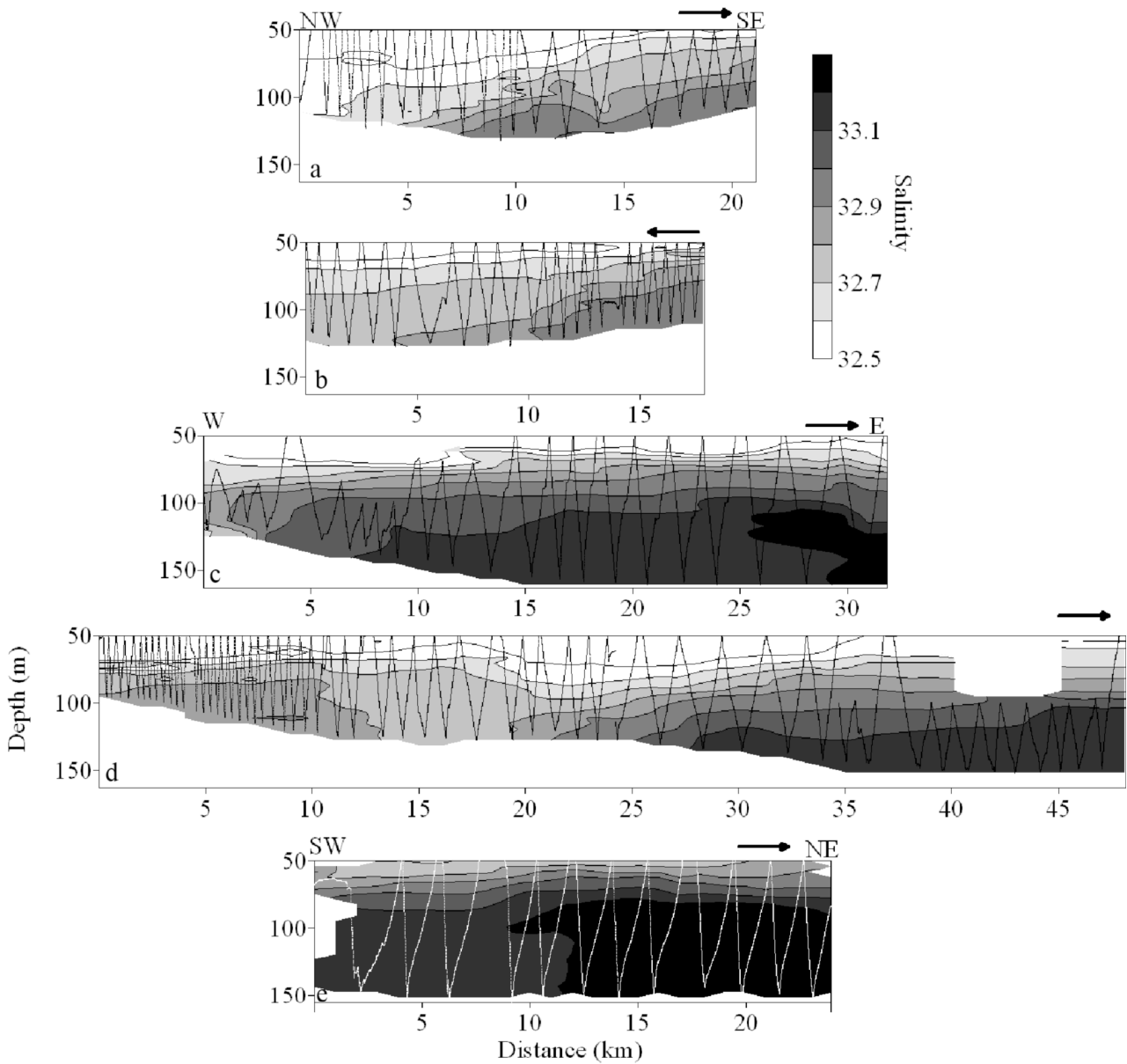


Fig. S11. Sectional distribution of salinity, estimated using the TUBSS-mounted Seabird-37 CTD in September 2008 in Roseway Basin (a, b) along the NW to SE transects-6 and -7, (c, d) along the W to E transects-8 and -9, and (e) SW to SE along transect-10. Arrows on each panel denote the direction of the tow, and zigzagged lines show the TUBSS tow profile. Transect line locations are depicted in Fig. 1 in the main text

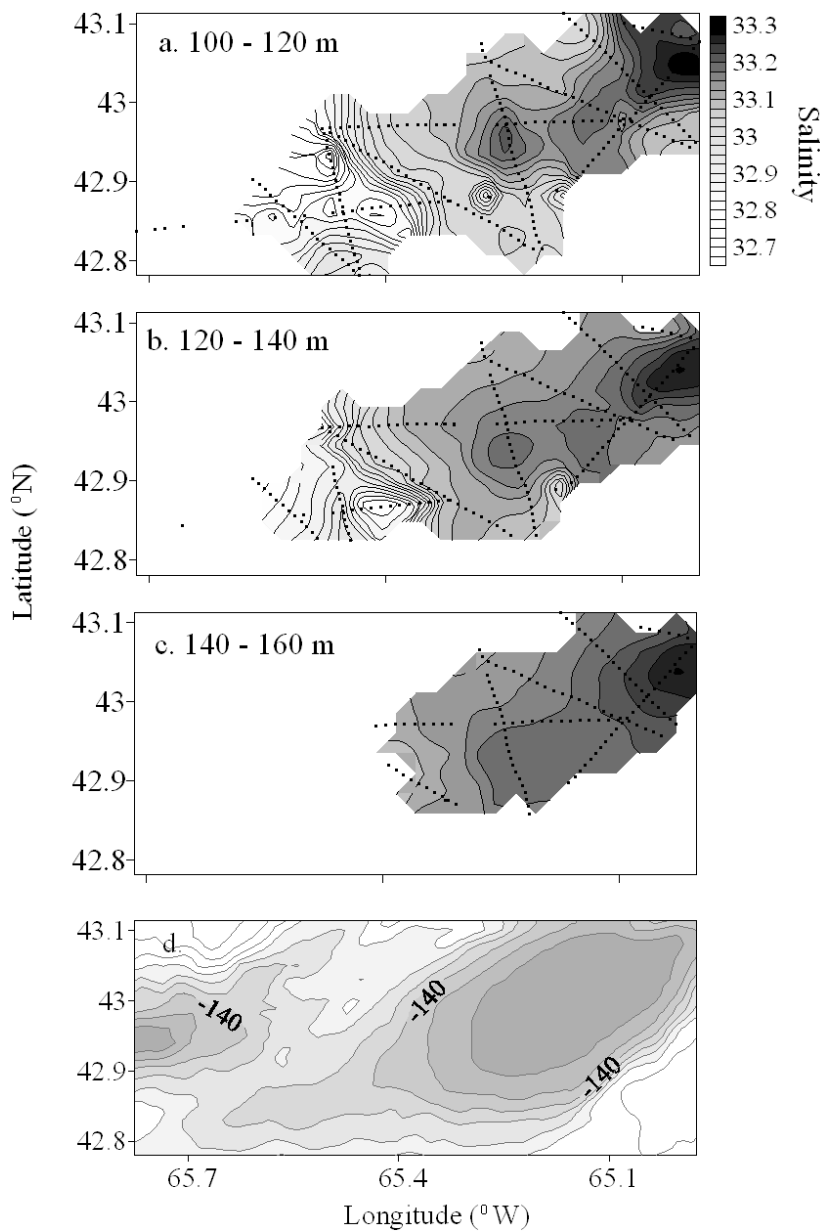


Fig. S12. Planar distribution of averaged integrated water mass salinity in September 2008 in the Roseway Basin over (a) the 100–120 m stratum, (b) the 120–140 m stratum, and (c) the 140–160 m stratum, and (d) the bathymetry of the Basin contoured at 10 m intervals with the 140 m contour labeled. The data were derived from each transect (see Figs. S6 and S7). Data points are indicated with black dots. Where data points are depicted without contours under them, data were insufficient to make an interpolation

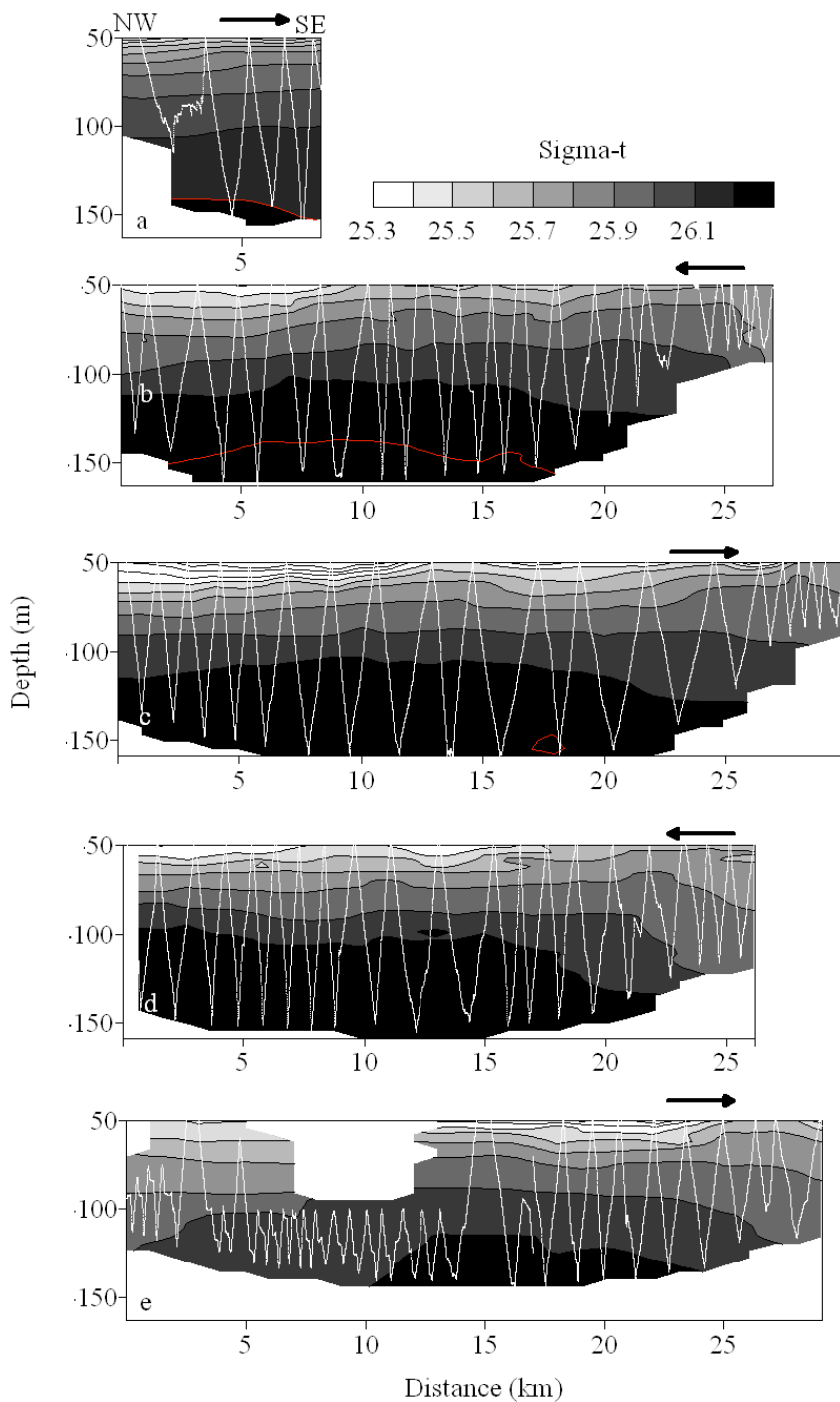


Fig. S13. Sectional distribution of water density ( $\sigma_t$ ,  $\text{kg m}^{-3}$ ), estimated using the TUBSS-mounted Seabird-37 CTD in September 2008 in Roseway Basin along the NW to SE transects-1 through -5 (panels a through e). Arrows on each panel denote the direction of the tow, and zigzagged lines show the TUBSS tow profile. Transect line locations are depicted in Fig. 1 in the main text. The 26.2  $\text{kg m}^{-3}$  isopycnal is depicted with a red line for clarity

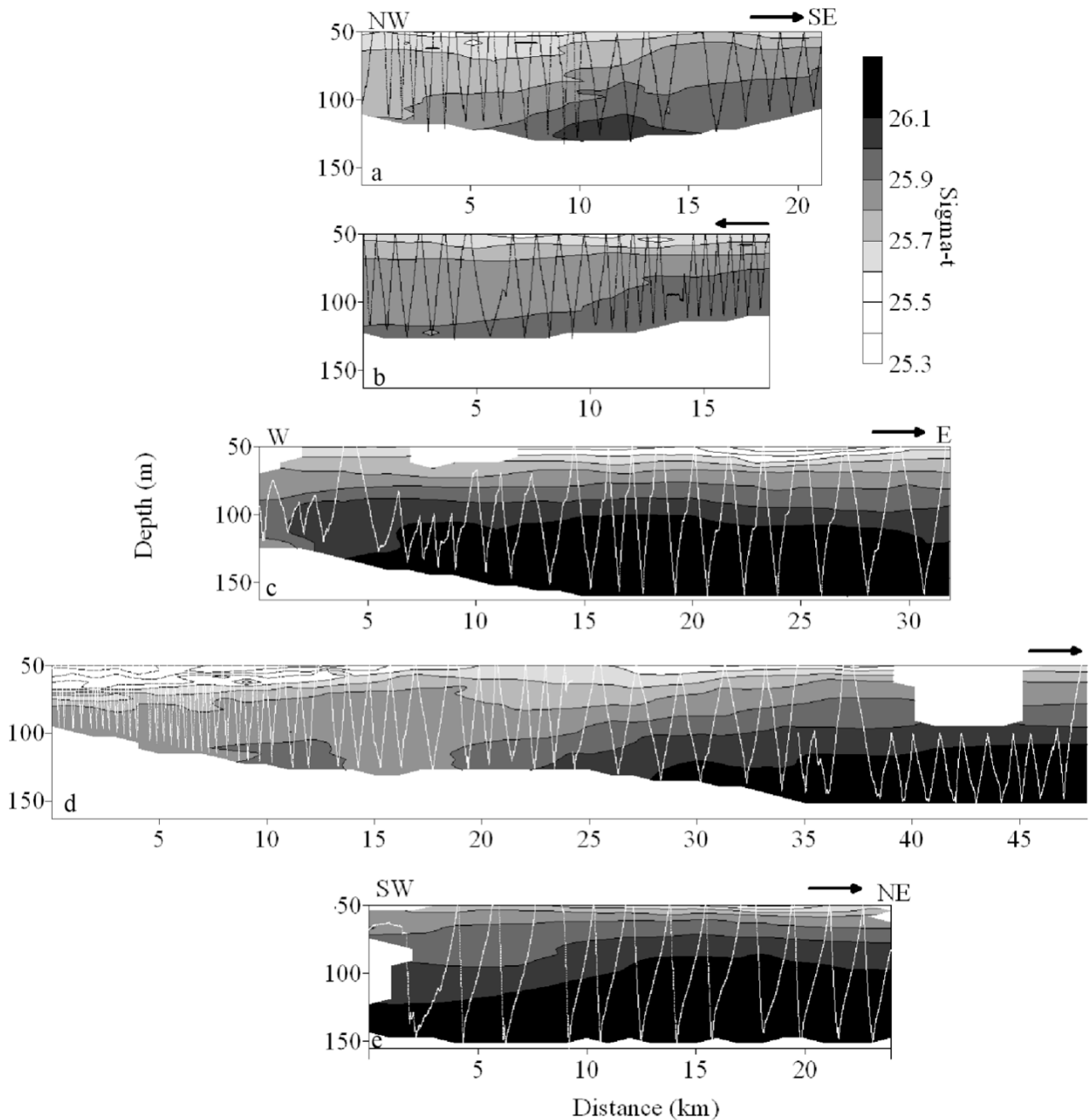


Fig. S14. Sectional distribution of water density ( $\sigma_t$ ,  $\text{kg m}^{-3}$ ), estimated using the TUBSS-mounted Seabird-37 CTD in September 2008 in Roseway Basin (a, b) along the NW to SE transects-6 and -7, (c, d) along the W to E transects-8 and -9, and (e) SW to SE along transect-10. Arrows on each panel denote the direction of the tow, and zigzagged lines show the TUBSS tow profile. Transect line locations are depicted in Fig. 1 in the main text